For Reference

NOT TO BE TAKEN FROM THIS ROOM

Thesis
1970
117

For Reference

NOT TO BE TAKEN FROM THIS ROOM

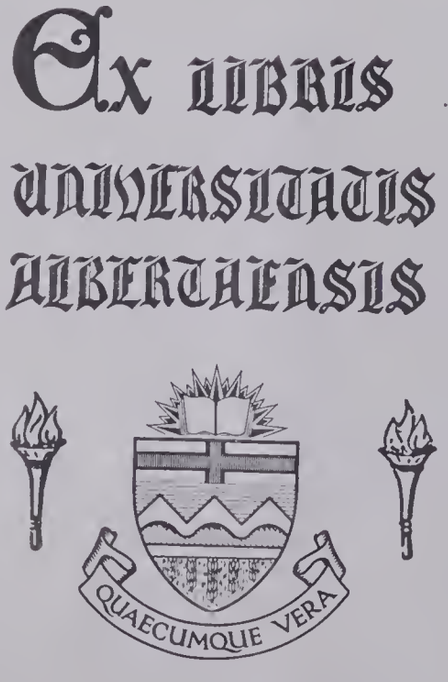

The University of Alberta
Printing Department
Edmonton, Alberta

THE UNIVERSITY OF ALBERTA

A STUDY OF THE MEASUREMENT OF ACCOMMODATION COEFFICIENTS

by

© D.J. SCHAFER, B.Sc. (ALBERTA)

A THESIS

SUBMITTED TO THE FACULTY OF GRADUATE STUDIES

IN PARTIAL FULFILMENT OF THE REQUIREMENTS FOR THE DEGREE

OF MASTER OF SCIENCE

DEPARTMENT OF MECHANICAL ENGINEERING

EDMONTON, ALBERTA

SPRING, 1970

Thesis
1970
117

UNIVERSITY OF ALBERTA

FACULTY OF GRADUATE STUDIES

The undersigned certify that they have read, and recommend to the Faculty of Graduate Studies for acceptance, a thesis entitled "A STUDY OF THE MEASUREMENT OF ACCOMMODATION COEFFICIENTS" submitted by DAVID JOHN SCHAFER in partial fulfilment of the requirements for the degree of Master of Science.

ABSTRACT

In this thesis a feasibility study is presented for the measurement of thermal and normal momentum accommodation coefficients. Two molecular number density detection systems are analysed: an ionization detector, and an electron flourescence device.

An analysis of experimental accuracy was carried out on the expression for the thermal accommodation coefficient. A one percent standard error in the measurement of the parameters was assumed to determine which measurements were most critical. The measurements which were found to be most critical were the number density in chamber A and the number density in the active zone of the detector.

The instrumentation was selected to minimize the error associated with the measurement of the most critical parameters.

The percent most probable error in the measurement of the thermal accommodation coefficient is less than six percent. The percent most probable error in the measurement of the normal momentum accommodation coefficient is less than five percent.

Both systems are well suited for measuring these accommodation coefficients.

ACKNOWLEDGEMENTS

The author wishes to extend his appreciation to Dr. D.J. Marsden for his guidance and supervision of this thesis. He also gratefully acknowledges the financial support received from the National Research Council and from the University of Alberta.

TABLE OF CONTENTS

LIST OF FIGURES

LIST OF SYMBOLS

A	area
$\bar{c}$	mean molecular speed
$\underline{c}$	velocity vector
c_m	most probable molecular speed
d	distance from the orifice to the active zone of the detector (centre of electron film or electron beam)
E	mean energy of molecules
F_{N_2}	fraction of nitrogen molecules present in chamber B
f	distribution function
G	geometric factor for the ionization detector
G_s	geometric factor for the electron flourescence device
I	output current from detector
K	calibration constant
$\underline{n}$	unit vector normal to unit area dA
n	molecular number density measured by detector
n_i	molecular number density in chamber A
n_{bg}	molecular number density in chamber B
n_s	molecular number density due to molecules effusing through the orifice
P	mean molecular normal momentum
P_A	pressure in chamber A
P_B	pressure in chamber B
r_o	radius of the orifice
S	standard deviation
T	temperature in degrees Kelvin

α	thermal accommodation coefficient
σ'	normal momentum accommodation coefficient
ϕ	angle between the flight path of a molecule and the normal unit vector of area A
ω	solid angle

SUBSCRIPTS

A	refers to chamber A
B	refers to chamber B
i	incident molecules
r	reflected molecules
s	molecules reflected with the surface temperature
bg	refer to background in chamber B

CHAPTER I

INTRODUCTION

Free molecular flow conditions exist when the mean free path of molecules in a gas is large compared to a characteristic dimension on a solid surface. Free molecular flow conditions exist in the atmosphere above an altitude of approximately 80 miles. In this ambient atmosphere, low orbiting earth satellites experience orbital decay due to the exchange of momentum between the atmospheric gas molecules and the satellite surface.

One of the earliest and most successful techniques for the measurement of thermal accommodation coefficient, α, is the conductivity cell method first introduced by Knudsen in 1910. The macroscopic heat transfer by free molecular conduction between a central electrically heated filament and a surrounding wall is measured directly to obtain the accommodation coefficient for the filament material.

Roberts was apparently the first to realize how important the effects of surface contamination can be, and in fact all measured values of accommodation coefficients are reliable only to the degree that the condition of the solid surface is known. One of the advantages of the conductivity cell method is that this relatively simple apparatus makes it easy to obtain clean metal surfaces by flash heating to evaporate contaminant gases. Some disadvantages are that the

range of solid surface materials is limited to conducting metal filaments, and that the solid surface temperature range is limited by radiation heat transfer effects which become large if the filament temperature is much above the temperature of the surroundings.

The conductivity cell method and results are discussed in a review paper by H.Y. Wachman (1).

More recent molecular beam techniques used by; Datz, Moore and Taylor, Smith and Fite, and others are described in a review by F.C. Hurlbut (2). This method is concerned with the scattering pattern of the reflected molecules. This method yields some microscopic behavior of the gas-surface interaction.

In this thesis, a feasibility study is made on a technique for measuring thermal and normal momentum accommodation coefficients. The vacuum system used for the experiment is designed to control impurity gases (thus surface contamination), and is designed so that any material (metallic or non-metallic) can be used for the test surface. Radiation effects do not limit the test surface temperature range.

The main concerns of this thesis are: the formulation of a complete error analysis, design of a device which monitors number density, and the selection of instrumentation required for the best possible accuracy. Two devices for monitoring the number density will be considered; an ionization detector and an electron flourescence device. The two systems will be compared, and the required system adaptations

will be cited.

1.1 Accommodation Coefficients

The normal momentum and energy transfer at a gas-solid interface are the quantities which can be determined by the experimental apparatus to be described in this thesis.

The average energy flux at a gas-solid interface is the difference between the energy of the incident molecules and the energy of the reflected molecules. The incident molecular stream and the reflected molecular stream may be considered independently if free molecular flow conditions exist. If the mean energy carried to the surface per incident molecule is ε_i (corresponding to temperature T_i), and if the number of molecules striking a unit area of the surface per unit time is N_i; then the total amount of energy, E_i, carried to the solid surface is $\varepsilon_i N_i$. Similarly, the amount of energy, E_r, leaving the solid surface is $\varepsilon_r N_r$ (corresponding to a temperature T_r, where $T_i \leq T_r \leq T_s$ if $T_s > T_i$). Therefore, the energy flux is $E_i - E_r$. If the gas-solid interaction were complete the temperature of the reflected molecules would be fully accommodated to the surface temperature, T_s. Hence, the energy flux in the completely accommodated case is $E_i - E_s$.

These two energy fluxes suggest that the average efficiency of the energy exchanged at a gas-solid interface can be expressed as a semi-emperical coefficient. This coefficient was defined by Knudsen in 1910 as the energy accommodation coefficient, α.

$$\alpha = \frac{E_i - E_r}{E_i - E_s} \qquad (1.1.1)$$

Similarly, the normal momentum accommodation coefficient, σ', can be defined as:

$$\sigma' = \frac{P_i - P_r}{P_i - P_s} \qquad (1.1.2)$$

Here the subscripts have the same meaning as in expression 1.1.1.

The above expression may be reduced to a more convenient form by assuming the velocity distribution of the reflected molecules to be Maxwellian. It can be shown that,

$$\alpha = \frac{T_i - T_r}{T_i - T_s} \qquad (1.1.3)$$

and,

$$\sigma' = \frac{(T_i)^{1/2} - (T_r)^{1/2}}{(T_i)^{1/2} - (T_s)^{1/2}} \qquad (1.1.4)$$

for a stationary gas in thermal equilibrium.

1.2 Vacuum System

The vacuum system used for the measurement of α and σ'

is described in detail in reference (3). Modifications will be cited in a later chapter.

For the sake of explanation, a schematic of the system is shown in Figure 1.3.1. The working pressure in the chamber A is maintained at 1×10^{-4} torr. The effective pumping speed from chamber B is 1900 litres per second. Chamber A and B are connected by a 2.08 mm diameter orifice which has a molecular conductance of 0.37 literes per second. From molecular flow theory, the pressure in chamber B should be approximately 1.95×10^{-8} torr.

The instrumentation will be cited in sections 2.5 and 3.5 after a complete error analysis has been carried out. The error analysis will enable us to determine the type and accuracy of instrumentation required.

The devices used for monitoring the number density of the molecular beam will also be discussed in sections 2.1 and 3.1.

1.3 Test Surface

According to Wachman (1), early investigators failed to specify the amount and type of contaminants present during the test. Thus the values of the accommodation coefficients reported are not reliable. To overcome this problem, a method used by J.J. Hinchen and E. Sheperd Malloy (6) was employed to clean the platinum test surface prior to the experimental run. Polycrystalline platinum targets are resistively heated in ultra high vacuum. This procedure cleans the surface by

oxide decomposition and causes the growth of large crystals with the <110> plane parallel to the test surface.

A platinum - 10% platinum, 90% rhodium thermocouple with a suitable millivolt readout can be used to measure the temperature of the surface. A 0.003 inch wire was used to avoid large heat loss by conduction along the thermocouple wire.

The temperature of the incident gas molecules is assumed to be equal to the wall temperature of chamber A. Chromel-alumel thermocouples together with a suitable potentiometer can be used to determine the wall temperature. The wall of chamber A can be kept at a constant uniform temperature by circulating water through the water jacket.

The test gas chosen was nitrogen because it does not chemisorb on platinum. Nitrogen has a well defined (0,0) band in the first negative system and is therefore well suited for the electron flourescence technique.

CHAPTER II

IONIZATION DETECTION

2.1 Description

The number density of the molecular beam will be measured by a device which is similar to the detection system designed by Hagena et al. (4) at the University of Virginia. This device mainly consists of three parts: (a) ionization chamber; (b) ion collector and (c) filament and shield. A schematic diagram of this detector is shown in Figure 2.1.1.

The ionization chamber was machined from stainless steel. The aperture, enabling the molecules to pass through the electron film, is covered by a 90% transparent stainless steel mesh. This mesh provides a uniform electric field to accelerate the positive ions towards the ion collector.

The ion collector consists of a stainless steel frame covered with 90% transparent mesh. The collector is mounted on the ionization chamber, opposite the entrance aperture. Teflon is used as the insulating material.

The filament shield arrangement is also mounted on the ionization chamber, but opposite the electron beam slits. This arrangement has the advantage that the cathode and anode may be interchanged by external switching. Electrons are produced by resistively heating the 0.010 inch tungsten filament. The filament and shield are insulated from the ionization chamber by alumina ceramic beads.

The electron film is collimated by a 900 gauss magnetic field. The permanent magnet supplying the field was enclosed in a stainless steel case to overcome outgassing.

2.2 Theory

Since the orifice connecting chambers A and B of the vacuum system has a diameter which is much less than the mean free path for nitrogen at a pressure of 10^{-4} torr. The number density at the detector can be calculated from the kinetic theory of gases.

The number of molecules with velocities between $\underline{c}$ and $\underline{c} + d\underline{c}$ is given by $f d\underline{c}$, where f is the distribution function. If the molecules are to cross an area $d\underline{A}$ in time dt, they must have occupied a volume $\underline{c}.\underline{n}\ dt\ dA$, where $\underline{n}$ is the unit vector normal to dA (Figure 2.2.1). Since $d\underline{c} = c^2 \sin\phi\ d\phi\ d\theta\ dc$, the number of molecules crossing dA in time dt with speeds between c and c + dc is:

$$c^3\ f\ dc\ d\theta\ \sin\phi\ \cos\phi\ d\phi\ dA\ dt$$

The number density in the active zone of the detector may be found by dividing the above expression by the volume swept out by the molecules in time dt.

$$dn_s = \frac{c^3\ f\ dc\ d\omega\ dA\ \cos\phi\ dt}{c\ \cos\phi'\ dA'\ dt} \qquad (2.2.1)$$

Therefore, the number of molecules passing between two surface areas, for a gas at rest in Maxwellian equilibrium, is found by determining $d\omega$.

$$d\omega = \frac{dA' \cos \phi'}{d^2/\cos^2 \phi}$$

Where ϕ is the angle between the molecular flight path and the normal of area dA. Substituting $d\omega$ into expression 2.2.1, we obtain;

$$dn_s = \frac{c^2 \, f \, dc \, dA \cos^3 \phi}{d^2}$$

since $\phi = \phi'$ for this detector.

The number density in the detector can be determined by integrating dn_s with respect to c. Hence,

$$n_s = \frac{\pi r_o^2}{d^2} \cos^3 \phi \int_0^\infty c^2 \, f \, dc = \frac{n_r r_o^2}{4d^2} \cos^3 \phi$$

where $A = \pi r_o^2$. If ϕ is small, then $\cos^3 \phi$ will approximately equal unity, giving

$$n_s = \frac{n_r r_o^2}{4d^2} \qquad (2.2.2)$$

In deriving expression 2.2.2, it was assumed that the reflected velocity distribution was Maxwellian. Logan and Stickney (5) have shown that the velocity distribution varies with the scattering angle. Hinchen and Malloy (6) compared Logan and Stickney's work to that of Harrison, who assumed the reflected velocity distribution was Maxwellian, and suggested that even if the velocity distribution is not Maxwellian, the error resulting from this assumption is very small.

The number of molecules incident on the surface must equal the number of molecules reflected. Hence,

$$\frac{n_i c_{mi}}{2(\pi)^{1/2}} = \frac{n_r c_{mr}}{2(\pi)^{1/2}}$$

where $c_m = (2RT)^{1/2}$ is the most probable molecular speed. This reduced to

$$\frac{T_r}{T_i} = \left(\frac{n_i}{n_r}\right)^2 . \qquad (2.2.3)$$

Since the detector is located in chamber B, there will be a background contribution to number density due to the pressure in this chamber. Therefore, the total number density, n, monitored by the detector will be the sum of the signal, n_s, and the background, n_{bg}.

$$n = n_s + n_{bg} \tag{2.2.4}$$

Substituting expression 2.2.2 into expression 2.2.4, we obtain n_r.

$$n_r = \frac{4d^2}{r_o^2} (n-n_{bg})$$

From expression 2.2.3 it can be shown that,

$$\frac{T_r}{T_i} = \left(\frac{r_o^2 n_i}{4d^2 (n-n_{bg})}\right)^2$$

Hence, the thermal accommodation coefficient may be written as,

$$\alpha = \frac{1 - \left[\frac{r_o^2 n_i}{4d^2 (n-n_{bg})}\right]^2}{1 - \frac{T_s}{T_i}} \tag{2.2.5}$$

and the normal momentum accommodation coefficient may be written as,

$$\sigma' = \frac{1 - \frac{r_o^2 n_i}{4d^2 (n-n_{bg})}}{1 - \left(\frac{T_s}{T_i}\right)^{1/2}} \tag{2.2.6}$$

2.3 Working Conditions

The pressure in chamber A is kept constant at 1×10^{-4} torr, corresponding to 3.37×10^{15} molecules per litre. From conductance and pumping speed relationships, the pressure in chamber B will be approximately 1.95×10^{-8} torr, corresponding to 6.55×10^{11} molecules per litre. The radius if the orifice is 0.1 cm and the distance d between the orifice and the active zone of the detector is 1.0 cm. Therefore, the geometric factor, $G = \frac{r_o^2}{4d^2}$, is 2.5×10^{-3}.

It would be useful to have upper and lower limits of number density in the active zone of the detector in order to determine the range of pressure, P_A, required for the calibration of the detector. If energy is completely accommodated, $T_r = T_s$ and $\alpha = 1$. Thus,

$$n = \frac{n_i r_o^2}{4d^2} \left(\frac{T_i}{T_s}\right)^{1/2} + n_{bg}$$

The maximum value of n will occur when $T_s = T_i$. Therefore, $n_{max} = 9 \times 10^{12}$ molecules per litre. The minimum value of n will occur when T_s is at its maximum value of 1293°K. Therefore, $n_{min} = 4.65 \times 10^{12}$ molecules per litre.

The pressure range required in chamber A may be determined from the following equations.

$$n = \frac{r_o^2}{4d^2} \frac{P_A}{kT_i} + n_{bg}$$

$$P_A = \frac{4d^2\ kT_i}{r_o^2}\ (n-n_{bg})$$

Substituting the values n_{max} and n_{min} for n, the pressure range is shown to be,

$$4.7 \times 10^{-5} \leq P_A \leq 1 \times 10^{-4} \text{ torr.}$$

The minimum value of the signal background ratio will be taken as n_{min}/n_{bg} which has a value of 6.1.

2.4 Analysis of Experimental Accuracy

An error analysis has been made to determine the variation in the accommodation coefficient when one parameter is varied.

The square of the standard deviation for a functional relationship is defined as (7),

$$S_u^2 = \sum_{j=1}^{n} (\delta u_j)^2/n$$

where

$$S_u = \left(\frac{\partial u}{\partial x}\right) \delta x_j + \left(\frac{\partial u}{\partial y}\right) \delta y_j + \ldots$$

Since $\left(\frac{\partial u}{\partial x}\right)$ $\left(\frac{\partial u}{\partial y}\right)$ will be equally likely to be positive as negative for large n, S_u^2 becomes

$$S_u^2 = \frac{(\frac{\partial u}{\partial x})^2 \sum_j^n (\delta x_j)^2 + (\frac{\partial u}{\partial y})^2 \sum_j^n (\delta y_j)^2 + \ldots}{n}$$

$$S_u^2 = (\frac{\partial u}{\partial x})^2 S_x^2 + (\frac{\partial u}{\partial y})^2 S_y^2 + \ldots \qquad (2.4.1)$$

where

$$S_x^2 = \sum_j^n \frac{(\delta x_j)^2}{n} = \sum_j^n \frac{(x_j - \bar{x})^2}{n}$$

We are assuming all errors are independent and may be treated as a normal distribution.

Redefining α by grouping parameters, we can write:

$$\alpha = \frac{1 - [\frac{Gn_i}{n-n_{bg}}]^2}{1 - \frac{T_s}{T_i}} \qquad (2.4.2)$$

Since the exact value for n which corresponds to a specific temperature ratio is not known, a value for n and T_s/T_i will be chosen within the expected range. Thus n is chosen as 6.65×10^{12} molecules per litre, and T_s/T_i as 2.0.

Applying expression 2.4.1 to equation 2.4.2, the square of the standard deviation in α is,

$$S_\alpha^2 = \left(\frac{\partial\alpha}{\partial G}\right)^2 S_G^2 + \left(\frac{\partial\alpha}{\partial n_i}\right)^2 S_{n_i}^2 + \left(\frac{\partial\alpha}{\partial n}\right)^2 S_n^2 \qquad (2.4.3)$$

$$+ \left(\frac{\partial\alpha}{\partial n_{bg}}\right)^2 S_{n_{bg}}^2 + \left(\frac{\partial\alpha}{\partial \frac{T_s}{T_i}}\right)^2 S_{\frac{T_s}{T_i}}^2$$

Differentiating expression 2.4.2 and substituting the appropriate values, we get:

$$\left|\frac{\partial\alpha}{\partial G}\right| = \frac{2Gn_i^2}{(n-n_{bg})^2\,(1-\frac{T_s}{T_i})} = 1.58 \times 10^3$$

$$\left|\frac{\partial\alpha}{\partial n_i}\right| = \frac{2G^2n_i}{(n-n_{bg})^2\,(1-\frac{T_s}{T_i})} = 11.7 \times 10^{-16}$$

$$\left|\frac{\partial\alpha}{\partial n}\right| = \frac{2G^2n_i^2}{(n-n_{bg})^3\,(1-\frac{T_s}{T_i})} = 6.56 \times 10^{-13}$$

$$\left|\frac{\partial\alpha}{\partial n_{bg}}\right| = \frac{2G^2n_i^2}{(n-n_{bg})^3\,(1-\frac{T_s}{T_i})} = 6.56 \times 10^{-13}$$

$$\left|\frac{\partial\alpha}{\partial \frac{T_s}{T_i}}\right| = \left(1 - \frac{G^2n_i^2}{(n-n_{bg})}\right)/(1-\frac{T_s}{T_i})^2 = 0.97$$

Squaring each of the above terms,

$$\left(\frac{\partial \alpha}{\partial G}\right)^2 = 2.5 \times 10^{6}$$

$$\left(\frac{\partial \alpha}{\partial n_i}\right)^2 = 1.37 \times 10^{-30} \qquad (2.4.4)$$

$$\left(\frac{\partial \alpha}{\partial n}\right)^2 = \left(\frac{\partial \alpha}{\partial n_{bg}}\right)^2 = 4.3 \times 10^{-25}$$

$$\left(\frac{\partial \alpha}{\partial \frac{T_s}{T_i}}\right)^2 = 0.94$$

To determine the sensitivity of α with respect to the parameters, the standard deviation in the measured values will be assumed to be one percent of their mean values. The results given in equations 2.4.6 below indicate the sensitivity of α to measuring accuracy for each parameter. Therefore, expression 2.4.1 yields:

$$S_x^2 = \frac{\sum_{j}^{n} (\delta x_i)^2}{n} = \frac{\sum_{j}^{n} (x_i - \bar{x})^2}{n} = (0.01\ \bar{x})^2$$

Hence:

$$S_G^2 = (\delta G)^2 = 6.25 \times 10^{-10}$$

$$S_{n_i}^2 = (\delta n_i)^2 = 11.35 \times 10^{26}$$

$$S_n^2 = (\delta n)^2 = 44.2 \times 10^{20} \qquad (2.4.5)$$

$$S_{n_{bg}}^2 = (\delta n_{bg})^2 = 42.9 \times 10^{18}$$

$$S_{\frac{T_s}{T_i}}^2 = (\delta \frac{T_s}{T_i})^2 = 4 \times 10^{-4}$$

Substituting expressions 2.4.4 and 2.4.5 into expression 2.4.3, the following square of the standard deviations associated with G, n_i, n, n_{bg} and T_s/T_i can be found.

$$(\frac{\partial \alpha}{\partial G})^2 S_G^2 = 1.56 \times 10^{-3}$$

$$(\frac{\partial \alpha}{\partial n_i})^2 S_{n_i}^2 = 1.56 \times 10^{-3}$$

(2.4.6)

$$(\frac{\partial \alpha}{\partial n})^2 S_n^2 = 1.90 \times 10^{-3}$$

$$(\frac{\partial \alpha}{\partial n_{bg}})^2 S_{n_{bg}}^2 = 1.84 \times 10^{-5}$$

$$\left(\frac{\partial \alpha}{\partial \frac{T_s}{T_i}}\right)^2 S_{\frac{T_s}{T_i}}^2 = 3.76 \times 10^{-4}$$

By summing the expressions in 2.4.6, the square of the standard deviation in α can be found (expression 2.4.3). This value yields the standard error in α, if all the measured values have an error of one percent. Hence, standard error = 0.0736, fractional standard error = $\frac{\text{standard error}}{\alpha}$ = 0.092, and fractional most probable error = (.675) (0.092) = 0.062 (fraction errors are based on α = 0.8).

Since errors in the measured parameters will, in all likelihood, not be equal to one percent, the square of the standard deviation in α can be determined by summing the product, $\left(\frac{\partial \alpha}{\partial x_i}\right)^2 S_{x_i}^2$, where S_{x_i} is determined for each measured parameter.

From expressions 2.4.6, it can be seen that the measurement of G, n_i, and n are most critical. A more rigorous analysis of the measurement of these parameters is made in the following section.

2.5 Evaluation of Measurement Accuracy

Instrumentation should be chosen so that the minimal experimental error can be achieved when measuring α and σ'..

2.5.1 Geometry Applying expression 2.4.1 to $G = \frac{r_o^2}{4d^2}$, we can write the square in the standard deviation in G as,

$$S_G^2 = \left(\frac{\partial G}{\partial r_o}\right)^2 S_{r_o}^2 + \left(\frac{\partial G}{\partial d}\right)^2 S_d^2$$

$$= \left(\frac{r_o}{2d^2}\right)^2 S_{r_o}^2 + \left(\frac{r_o^2}{2d^3}\right)^2 S_d^2 \qquad (2.5.1)$$

$$= 0.25 \times 10^{-2} S_{r_o}^2 + 0.25 \times 10^{-4} S_d^2$$

Since r_o and d are determined by a direct measurement, the square of the standard deviation in these measurements will be very small providing extreme care is taken (a large number of actual measurements should be made). Since r_o is machined and rigid, this measurement will have little error. We can assume,

$$S_{r_o}^2 = \frac{\sum_j^n (r_{o_j} - \bar{r}_o)^2}{n} = (0.0001\ r_o)^2 = 10^{-10}\ cm^2$$

Due to the difficulty in positioning the detector filament, the distance d will have to be measured a large number of times, and we will assume,

$$S_d^2 = \frac{\sum_j^n (d_j - \bar{d})^2}{n} = (0.0001\ d)^2 = 10^{-8}\ cm^2$$

Substituting the appropriate values into expression 2.5.1, the square of the standard deviation, S_G^2, is found to be 0.5×10^{-12}. The resulting uncertainty in α is $(\frac{\partial \alpha}{\partial G})^2 S_G^2 = 1.25 \times 10^{-2}$.

2.5.2. Temperature The measurement of temperature is not critical except when T_s/T_i approaches unity. This singularity should be noted and if measurements are made in this temperature range it must be considered.

Following an analysis similar to that in 2.5.1, let $T = T_s/T_i$, and the expression 2.4.1 becomes,

$$S_T^2 = (\frac{\partial T}{\partial T_s})^2 S_{T_s}^2 + (\frac{\partial T}{\partial T_s})^2 S_{T_i}^2$$

$$= (\frac{1}{T_i})^2 S_{T_s}^2 + (\frac{-T_s}{T_i^2})^2 S_{T_i}^2 \qquad (2.5.2)$$

The temperature measurements are made with a Leeds Northrup Potentiometer. This millivolt readout has a resolution of 0.005 millivolts which corresponds to less than 2°C. Therefore S_{T_s} and S_{T_i} can be chosen as 2°C, and T chosen as 2 (i.e., $T_s = 580$°C and $T_i = 290$°C). Substituting the above values into expression 2.5.2, we find S_T^2 is 2.38×10^{-4}. The resulting uncertainty in α is $(\frac{\partial \alpha}{\partial T})^2 S_T^2 = 2.24 \times 10^{-4}$.

2.5.3. Pressure Gauges

2.5.3.1. Pressure in Chamber A From section 2.4, it is seen that the measurement of n_i is critical. The instrumentation chosen to monitor this pressure must have a high degree of stability. For this reason, a MKS Baratron Model 90H-3 pressure transducer was chosen to monitor the pressure in chamber A. The manufacturers claim this gauge has a long term drift of less than one percent after warming up.

One additional advantage of this gauge is that it is a direct pressure measuring device. It is a diaphram type pressure transducer which is calibration against a change in capacitance. Thus, there are no hot filaments to cause degassing from the surrounding structure which may supply impurity gases to contaminate the platinum test surface.

2.5.3.2. Background Pressure A Varian partial pressure gauge model 974-0036, which has a long term drift of less than one percent, can be used for monitoring the pressure in chamber B. The amounts of impurity gases present will also be measured with this gauge. The length of time the test surface will remain atomically clean can be determined from the knowledge of the amounts of impurity gases.

2.5.4. Ionization detector The detection system described in section 2.1 is used for the measurement of n. The instrumentation required for measuring the electron film current must have very little long term drift. A Varian dual range ionization gauge control unit model 971-0014 can

be adapted for this purpose.

The control unit grid is attached to the detector shield which corresponds to the electron collector (anode). The potential of the anode is +175 volts. The filament shield assembly, which is the electron emission side, is at a potential of +45 volts and connected directly to the control unit. The ion collector is also connected directly to the control unit at ground potential. The ionization chamber is set at +125 volts by a highly regulated Harrison Laboratories 6209B DC power supply.

A simple schematic for this circuit is shown in Figure 2.1.1. The accelerating potentials are shown to provide insight in the functioning of the detector. This control unit provides feedback on emission current which stabilizes it. This feedback is needed to stabilize the emmission current for accurate calibration.

Referring to equation 2.2.4 for the number density measured by the detector, we obtain:

$$n = Gn_i + n_{bg} \tag{2.5.3}$$

and applying expression 2.4.1 to the above equation; the actual square of the standard deviation is obtained,

$$S_n^2 = \left(\frac{\partial n}{\partial G}\right)^2 S_G^2 + \left(\frac{\partial n}{\partial n_i}\right)^2 S_{n_i}^2 + \left(\frac{\partial n}{\partial n_{bg}}\right) S_{n_{bg}}^2$$

$$= n_i^2 S_G^2 + G^2 S_{n_i}^2 + S_{n_{bg}}^2$$

Substituting the appropriate values from section 2.4 and 2.5, we find $S_n^2 = 71.5 \times 10^{20}$. Therefore the square of the standard deviation, $(\frac{\partial \alpha}{\partial n})^2 S_n^2$, associated with the uncertainty in n is equal to 3.07×10^{-3}. This error is slightly more than an error one percent, and it is due to measurement of n_i - in particular S_{n_i} is too large.

Since n is measured in terms of an output current, the error involved during calibration must be considered. From Hagena (4), the equation for the output current is given as:

$$I = k \cdot i_{eff} \cdot l_{eff} \cdot \sigma_{eff} \cdot n \qquad (2.5.4)$$

where

k is the amplification

i_{eff} is the effective electron current

l_{eff} is the effective electron flight path

σ_{eff} is the effective collision cross section for a nitrogen molecule and an electron.

Once the system is set in the working condition described previously, equation 2.5.4 reduces to:

$$I = Kn \qquad (2.5.5)$$

where K is a calibration constant.

Since this calibration has not been done, we will assume a value for K to clarify the illustration. We expect the input current to be small, in the order of nanoamps, but the degree of amplification will increase the input current

to the order of microamps. Hence, I may be speculated to be 5×10^{-6} amps when $n = 6.65 \times 10^{12}$ molecules per litre. Therefore, K is equal to 7.5×10^{-19} amp-litre.

Rearranging expression 2.5.5, we have:

$$K = \frac{I}{n} \tag{2.5.6}$$

Applying expression 2.4.1 to equation 2.5.6

$$S_K^2 = \left(\frac{\partial K}{\partial I}\right)^2 S_I^2 + \left(\frac{\partial K}{\partial n}\right)^2 S_n^2$$

$$= \frac{1}{n^2} S_I^2 + \frac{I^2}{n^4} S_n^2$$

where S_I is one percent of I. Substituting the correct values, we find the standard deviation in K is 1.22×10^{-20}, and the percent standard error is 1.65%. If the points plotted on the I verses n graph are all within $\pm$ 1.65% of the best fit curve, then the value of n as determined during the test will have the desired accuracy. If the spread of points on the I verses n plot is greater than $\pm$ 1.65% of the best fit curve, then adjustments in the control unit, and readout device must be made.

The critical measurements in the system are n_i and n. The pressure in chamber A must remain constant throughout the test run. Accurate pressure measurements can be obtained

with the aid of a recorder which will provide greater accuracy than a panel meter, even if there are no fluctuations in the signal to be averaged. Increased sensitivity can be obtained by use of an offset bias voltage with the recorder.

2.6 Experimental Procedure

Although the number densities have to be measured accurately to obtain an accurate value of the accommodation coefficient, it will not be necessary to have the absolute value of n_i to the same degree of accuracy because the number density appears in the equation for α as a ratio $\frac{n_i}{n - n_{bg}}$. The units of the calibration are not important and hence the absolute calibration is not critical. Absolute values of n_i are primarily required to determine if the experiment is in the free molecule flow regime.

The ratio, $\frac{n_i}{n - n_{bg}}$, yields a simple method for calibrating the detector. The pressure in the chamber A may be assumed correct, enabling n and n_{bg} to be calibrated against n_i by using molecular flow theory.

$$P_B = \frac{C}{C + S} P_A \qquad (2.6.1)$$

$$n = \frac{r_o^2}{4d^2} \frac{P_A}{kT_i} + \frac{C}{C + S} \frac{P_A}{kT_{bg}} \qquad (2.6.2)$$

P_A may be increased in increments from 4×10^{-5} to

1×10^{-4} torr. At each increment P_A, P_B and I should be allowed to reach equilibrium before the readings are recorded. During calibration T_s is kept constant at the wall temperature, T_i.

A plot of n_i versus n_{bg} can be made using expression 2.6.1. Also from expression 2.5.5 and 2.6.2, a plot of I versus $n = n(P_A)$ can be made to determine K as discussed in section 2.5.

This calibration procedure will yield a method for determining α, since once I is recorded the ratio is known. A plot of I versus $n_i/n-n_{bg}$ can be made for added convenience. In this case, n_i would be the working number density which remains constant during the test run, n and n_{bg} are the experimental values.

During the test run the pressure in chamber A is maintained at 1×10^{-4} torr with the aid of a Granville-Phillips automatic pressure controller. The surface temperature is increased and the readout current, I, and pressure, P_B, are recorded for each temperature station.

A plot of I versus T_s/T_i can be presented to show the variation of number density as a function of surface temperature. A plot of α and σ' versus T_s/T_i will exhibit the change in α and σ' with variation of the surface temperature.

CHAPTER III

ELECTRON FLOURESCENCE DETECTOR

3.1 Description

The electron beam technique used to measure the number density of nitrogen, at point P in chamber B (see Figure 3.1.2), is an extension of a technique developed by E.O. Gadamer (8). E.P. Muntz (9), D.J. Marsden (10) and others at UTIAS.

When a high energy electron collides with a nitrogen molecule which is in the N_2 $X^1 \sum_g^+$ ground state, the molecule is ionized and electronically excited to the N_2 B $\sum_u^+$ state. A photon of light is emitted when the excited molecule makes a spontaneous transition to the N_2^+ $X^2 \sum_g^+$ state. This series of transitions gives rise to the first negative system in the nitrogen emission spectrum (9).

The electron gun used for this detector is Phillips 902-564 television gun. The aiming system for the electron gun is designed to allow rotational and translational alignments.

The electron gun incorporates electrostatic lenses for focussing the beam. A 1.5 millimeter diameter aperture, located about 3 inches from point P, is used to collimate the electron beam.

The power supply for operating the electron gun is a N.J.E. 0-30 KV, 0.0 - 2.0 ma. The normal operating voltage

is 10 KV, and the maximum gross beam current is about one ma. The actual beam current is monitored by a millimeter.

The flourescence light output is monitored by a E.M.I. 9205 S Photomultiplier. The photomultiplier power supply is a Fluke, model 410B, 0-2.1 KV which has a high degree of regulation. The photocurrent is measured by a Kiethly Instruments, 610 B electromenter.

A more detailed description of the electron floure-scence detector, and its operation is given in reference (3). Figure 2.1.1 also shows the basic optical features of this device.

3.2 Theory

The light reaching the photomultiplier is limited, to the flourescence from the N_2^+ (0,0) band of the nitrogen ion, by means of an interference filter which only passes light within a narrow range of wavelengths centred around 3900 Angstrom units.

The number density of nitrogen is made up of two parts: signal and background. Hence, we may write the number density of nitrogen at point P (see Figure 3.2.1) as,

$$n = n_s + n_{bg} \qquad (3.2.1)$$

where n_s is the contribution to the number density of nitro-gen at point P due to molecules effusing through the orifice in solid angle $d\omega_s$ and n_{bg} is the contribution to the number density of nitrogen at point P due to the partial pressure

of nitrogen in chamber B. If the number density of the gas in chamber B is n_B, then n_{bg} may be determined from the mass spectrometer scan and the total pressure in chamber B. Therefore,

$$n_{bg} = \frac{\text{peak height of } N_2^+}{\sum \text{ all peak heights}} \times n_B \ (1-G_s)$$

$$n_{bg} = F_{N_2} \ (1-G_s) \ n_B \qquad (3.2.2)$$

where G_s is a geometric factor.

The signal number density is determined from the following analysis.

$$n_s = n_r \frac{d\omega_s}{4\pi} \qquad (3.2.3)$$

The solid angle $d\omega_s$ is calculated as follows:

$$d\omega_s = \int_0^{2\pi} \int_0^{r_o} \frac{r \ dr \ d\theta}{r^2 + d^2}$$

$$d\omega_s = \pi \ \ln \left(\frac{r_o^2 + d^2}{d^2}\right) \qquad (3.2.4)$$

$$G_s = \frac{d\omega_s}{4\pi} = \frac{1}{4} \ln \left(\frac{r_o^2 + d^2}{d^2}\right)$$

where r_o = 0.1 cm is the radius of the orifice and d = 1 cm is the perpendicular distance between the orifice and the electron beam. Substituting the appropriate values, G_s is equal to 0.00249. Hence, 1 - G_s is approximately equal to 1.0.

The number density of nitrogen at point P may be determined by substituting expressions 3.2.2, 3.2.3, and 3.2.4 into expression 3.2.1.

$$n = G_s\, n_r + F_{N_2}\, n_B \qquad (3.2.5)$$

$$n_r = \frac{1}{G_s}\,(n - F_{N_2}\, n_B)$$

Using expression 2.2.3, we get

$$\frac{T_r}{T_i} = \left(\frac{n_i}{n_r}\right)^2 = \left(\frac{G_s\, n_i}{(n - F_{N_2}\, n_B}\right)^2 \qquad (3.2.6)$$

Substituting expression 3.2.6 into expression 1.2.3, the thermal accommodation coefficient may be written as,

$$\alpha = \frac{1 - \left(\frac{G_s\, n_i}{n - F_{N_2}\, n_B}\right)^2}{1 - \frac{T_s}{T_i}} \qquad (3.2.7)$$

And from expression 1.2.4, the normal momentum accommodation coefficient may be written as,

$$\sigma' = \frac{1 - \left(\frac{G_s\, n_i}{n - F_{N_2}\, n_B}\right)}{1 - \left(\frac{T_s}{T_i}\right)^{1/2}} \qquad (3.2.8)$$

3.3 Working Condition

The upper and lower limits of the number density of nitrogen at point P will enable us to determine the required calibration pressure range in chamber A. If energy is completely accommodated $T_r = T_s$ and α equals 1.0. From expression 3.2.6, we can write:

$$n = G_s\, n_i \left(\frac{T_i}{T_r}\right)^{1/2} + F_{N_2}\, n_B \qquad (3.3.1)$$

where G_s is 0.00249, n_i is 3.37×10^{15} molecules per litre, and $n_{bg} = F_{N_2}\, n_B$ is 6.55×10^{11} molecules per litre. The value of n_{bg} is only approximate, but can be determined correctly when the apparatus is operating.

Substituting the appropriate values into expression 3.3.1, we find $n_{max} = 7.96 \times 10^{12}$ molecules per litre when $T_r = 293°K$, and $n_{min} = 4.13 \times 10^{-2}$ molecules per litre when $T_r = 1293°K$.

Therefore, the approximate pressure range required for calibration is,

$$4.7 \times 10^{-5} \leq P_A \leq 1 \times 10^{-4} \text{ torr}$$

The theoretical signal background ratio will be taken as n_{min}/n_{ng} and has a value of 5.3. However, this value neglects stray light in the system and the dark current of the photomultiplier which will make up part of the background signal.

3.4 Analysis of Experimental Accuracy

An error analysis similar to the one completed in section 2.4 will be followed in this section. Hence, expression 2.4.1 may be written as,

$$S_\alpha^2 = \left(\frac{\partial\alpha}{\partial G_s}\right)^2 S_{G_s}{}^2 + \left(\frac{\partial\alpha}{\partial n_i}\right)^2 S_{n_i}{}^2 + \left(\frac{\partial\alpha}{\partial n}\right)^2 S_n{}^2 + \left(\frac{\partial\alpha}{\partial n_{bg}}\right)^2 S_{n_{bg}}{}^2 + \left(\frac{\partial\alpha}{\partial \frac{T_s}{T_i}}\right)^2 S_{\frac{T_s}{T_i}}{}^2 \qquad (3.4.1)$$

where n is 6.65×10^{12} molecules per litre and T_s/T_i is 2.0. Values for n and T_s/T_i have been chosen within the expected range.

Differentiating expression 3.2.7 with respect to each parameter, we obtain,

$$\left|\frac{\partial\alpha}{\partial G_s}\right| = \frac{2n_i{}^2\, G_s}{(n-n_{bg})^2\,(1-\frac{T_s}{T_i})} = 1.58 \times 10^3$$

$$\left|\frac{\partial\alpha}{\partial n_i}\right| = \frac{2n_i\, G_s^2}{(n-n_{bg})^2\ (1-\frac{T_s}{T_i})} = 11.7 \times 10^{-16}$$

$$\left|\frac{\partial\alpha}{\partial n}\right| = \frac{2n_i^2\, G_s^2}{(n-n_{bg})^3\ (1-\frac{T_s}{T_i})} = 6.56 \times 10^{-13}$$

$$\left|\frac{\partial\alpha}{\partial n_{bg}}\right| = \frac{2n_i^2\, G_s^2}{(n-n_{bg})^3\ (1-\frac{T_s}{T_i})} = 6.56 \times 10^{-13}$$

$$\left|\frac{\partial\alpha}{\partial\frac{T_s}{T_i}}\right| = \frac{1 - (\frac{G_s n_i}{n-n_{bg}})^2}{(1-\frac{T_s}{T_i})^2} = 0.97$$

Squaring each of the above terms,

$$(\frac{\partial\alpha}{\partial G_s})^2 = 2.5 \times 10^{6}$$

$$(\frac{\partial\alpha}{\partial n_i})^2 = 1.37 \times 10^{-30}$$

(3.4.2)

$$(\frac{\partial\alpha}{\partial n})^2 = (\frac{\partial\alpha}{\partial n_{bg}})^2 = 4.3 \times 10^{-25}$$

$$(\frac{\partial\alpha}{\partial\frac{T_s}{T_i}})^2 = 0.94$$

To determine the sensitivity of α to each parameter, the standard deviation in the measured values will be set at one percent. Thus, expression 2.4.1 yields:

$$S_x^2 = \frac{\sum_i (\delta x_i)^2}{n} = \frac{\sum_i (x_i - \bar{x})^2}{n} = (0.01\ \bar{x})^2$$

hence,

$$S_{G_s}^2 = 6.25 \times 10^{-10}$$

$$S_{n_i}^2 = 11.35 \times 10^{26}$$

$$S_n^2 = 44.2 \times 10^{20}$$

$$S_{n_{bg}}^2 = 42.9 \times 10^{18}$$

$$S_{\frac{T_s}{T_i}}^2 = 4.0 \times 10^{-4}$$

The sensitivity of α, due to variations in parameters, is determined by expression 3.4.1;

$$\left(\frac{\partial \alpha}{\partial G_s}\right)^2 S_{G_s}^2 = 1.56 \times 10^{-4}$$

$$\left(\frac{\partial \alpha}{\partial n_i}\right)^2 S_{n_i}^2 = 1.56 \times 10^{-3}$$

$$\left(\frac{\partial \alpha}{\partial n}\right)^2 S_n^2 = 1.9 \times 10^{-3}$$

$$\left(\frac{\partial \alpha}{\partial n_{bg}}\right)^2 S_{n_{bg}}^2 = 1.84 \times 10^{-5} \qquad (3.4.3)$$

$$\left(\frac{\partial \alpha}{\partial \frac{T_s}{T_i}}\right)^2 S_{\frac{T_s}{T_i}}^2 = 3.76 \times 10^{-4}$$

By summing the expressions in 3.4.3, the square of the standard deviation in α can be determined (expression 3.4.1). This value yields the standard error in α, if all the measured values have an error of one percent. Hence,

$$\text{Standard error} = 0.0552$$

$$\text{Fractional standard error} = \frac{\text{standard error}}{\alpha} = .069$$

$$\text{Fractional most probable error} = (0.675)(0.069) = 0.046$$

From expression 3.4.3, it can be seen that the measurement of G, n_i and n are most critical. A more rigorous analysis of these parameters is made in the following section.

3.5 Evaluation of Measurement Accuracy

Since the vacuum system used is identical to the system

used in Chapter II, some of the instrumentation associated with the electron flourescence detector is identical to the instrumentation used for the ionization detector. Errors associated with this previously considered instrumentation will be repeated for completeness.

3.5.1 Geometry To insure the correct error in α is known, a more rigorous treatment of the geometric factor, G_s, should be made. Applying expression 2.4.1 to $G_s = \frac{1}{4} \ln \left(\frac{r_o^2 + d^2}{d^2}\right)$, we may write:

$$S_{G_s}^2 = \left(\frac{\partial G_s}{\partial r_o}\right)^2 S_{r_o}^2 + \left(\frac{\partial G_s}{\partial d}\right)^2 S_d^2$$

$$= \left(\frac{r_o}{2(r_o^2+d^2)}\right)^2 S_{r_o}^2 + \left(\frac{r_o^2}{2d(r_o^2+d^2)}\right)^2 S_d^2$$

$$= 25 \times 10^{-4} S_{r_o}^2 + 25 \times 10^{-6} S_d^2 \qquad (3.5.1)$$

As explained in section 2.4, $S_{r_o}^2$ has a value of approximately 10^{-10}.

The value of d is not so easily determined as in section 2.4. The distance d is the average distance between the orifice and the centre of the electron beam.

This distance can be measured with the aid of a CENCO No. 74002 measuring microscope made to replace the microscope objective of a No. 72905 measuring microscope. This

adaption will convert the microscope to a cathetometer with a focusing range from 60 cm. to infinity. The cathetometer can be mounted on a height gauge equipped with a vernier capable of reading to 0.01 mm.

The cathetometer can be focused at the elevation of the orifice (bottom of chamber A). Then it can be lowered, and focused on the electron beam. The difference in the two readings is the distance d.

The pressure in chamber B will have to be raised to approximately 10^{-4} torr before the light intensity emitted from the electron beam becomes visible.

The centre of the beam will be easily determined since the beam diameter is only 1 mm and light is most intense at the centre. An estimate of the square of the standard deviation in d is assumed to be $(.001\ \bar{d})^2$ cm^2.

Substituting values into expression 3.3.4 we find $S_{G_s}{}^2$ equals 25.25×10^{-12}. Therefore, $(\frac{\partial \alpha}{\partial G_s})^2\ S_{G_s}{}^2 = 6.3 \times 10^{-5}$ which is the sensitivity of α due to measurement uncertainties in geometry. This is less than half the value of 15.6×10^{-5} obtained assuming one percent accuracy in measurements.

3.5.2 Temperature As described in sub-section 2.5.2 the square of the standard deviation in α associated with T_s/T_i is $(\frac{\partial \alpha}{\partial \frac{T_s}{T_i}})^2\ S_{\frac{T_s}{T_i}}{}^2 = 2.24 \times 10^{-4}$. This error is due to the resolution of the Leeds-Northrup Potentiometer.

3.5.3 Pressure Gauges

3.5.3.1 Pressure in Chamber A The square of the standard deviation in association with n_i is $(\frac{\partial \alpha}{\partial n_i})^2 S_{n_i}^2 = 1.56 \times 10^{-3}$. This error is due to the one percent long term drift of the MKS Baratron gauge.

3.5.3.2 Background Pressure Since n_{bg} is the partial pressure of nitrogen in chamber B, an analysis should be completed to determine the error involved. Applying expression 2.4.1 to $n_{bg} = F_{N_2} n_B$, we can write,

$$S_{n_{bg}}^2 = (\frac{\partial n_{bg}}{\partial F_{N_2}})^2 S_{F_{N_2}}^2 + (\frac{\partial n_{bg}}{\partial n_B})^2 S_{n_B}^2$$

$$= n_B^2 S_{F_{N_2}}^2 + F_{N_2}^2 S_{n_B}^2 \qquad (3.5.2)$$

A value for F_{N_2} (fraction of nitrogen molecules present in chamber B) may be obtained from Figure 7 in reference (3). This value is found to be 0.965. An estimate of the standard error in F_{N_2} was found from the same plot by noting the point scatter around the best fit curve. This error was calculated to be 1.5 percent of the slope. Therefore, $S_{F_{N_2}}^2 = (0.015\ F_{N_2})^2$ and $F_{N_2} = 0.965$. Values for n_B and $S_{n_{bg}}^2$ are taken from section 3.4. Substituting into expression 3.5.2, we can calculate $S_{n_{bg}}^2$ to equal 9.2×10^{17} and $(\frac{\partial \alpha}{\partial n_{bg}})^2 S_{n_{bg}}^2$

is 3.96×10^{-7}. This error is not significant when compared to errors associated with the measurement of n_i.

3.5.4 Electron Flourescence Detector This detection system, which is described in section 3.1, is used to monitor the number density of nitrogen at point P_A description of the electronics, operation, and calibration of this detection system is given in reference (3).

Following a parallel analysis presented in sub-section 2.5.4, we can write the equation for the square of the standard deviation in n. Therefore, using expression 3.2.5, we get:

$$S_n^2 = \left(\frac{\partial n}{\partial G}\right)^2 S_{G_s}^2 + \left(\frac{\partial n}{\partial n_i}\right)^2 S_{n_i}^2 + \left(\frac{\partial n}{\partial n_{bg}}\right)^2 S_{n_{bg}}^2 \qquad (3.5.3)$$

differentiating,

$$S_n^2 = n_i^2 S_{G_s}^2 + G_s^2 S_{n_i}^2 + S_{n_{bg}}^2$$

substituting the appropriate values from section 3.4 and 3.5, we find $S_n^2 = 7.4 \times 10^{21}$ and $\left(\frac{\partial \alpha}{\partial n}\right)^2 S_n^2 = 3.18 \times 10^{-3}$. The sensitivity of α, associated with the measurement of n is significant when compared to the magnitudes of the sensitivities for the other parameters. S_n^2 is large solely because $S_{n_i}^2$ is large, even though $S_{n_i}^2$ can be measured within a one percent standard error.

Since n is measured in terms of an output current, the error involved during calibration must be considered. In reference (10), the emission intensity is given by,

$$I' = n' \, hc \, \nu \, A_{nm} \qquad (3.5.4)$$

where

n' = the number density of the molecules in the excited state at any instant

h = planck's constant

c = velocity of light

ν = the wave number of the light emitted

A_{nm} = Einstein's spontaneous emission probability

The depopulation of the excited state by spontaneously emitting radiation per second is $n'A_{nm}$ and the depopulation of the excited state by the collisions with neutral molecules per second is $2n'n \, \delta^2 \, (4\pi RT)^{1/2}$ (see reference (10)). Hence,

$$F.n = n'A_{nm} + 2n'n \, \delta^2 \, (4\pi RT)^{1/2} \qquad (3.5.5)$$

where,

n = number density of the gas

F = fraction of n excited by the electron beam per second

δ = effective radius of the collision cross section

Therefore,

$$n' = \frac{F.n}{A_{nm} + 2n\,\delta^2\,(4\pi RT)^{1/2}} \qquad (3.5.6)$$

Substituting equation 3.5.6 into equation 3.5.4, we can write:

$$I' = \frac{F.n\,hc}{(1 + 2n\,\delta^2\,(4\pi RT)^{1/2}/A_{nm})} \qquad (3.5.7)$$

The quenching collision term is not significant if

$$2n\,\delta^2\,(4\pi RT)^{1/2}/A_{nm} << 1$$

and since $n = 6.65 \times 10^{12}$ per litre, the quenching term is not significant. Therefore,

$$I' = F.h.c.n \qquad (3.5.8)$$

or

$$I = k\,n$$

where,

I = the output current of the photomultiplier

K = a calibration constant

This constant has been determine in reference (3), which also cites the factors incorporated in it. The value of K was found to be 4.1×10^{-5} Amp/torr which corresponds to 1.24 x

10^{-24} Amp-litre.

Following a parallel analysis as presented in sub-section 2.4.3, the desired accuracy in K can be found. Applying expression 2.4.1 to K = I/n, we can write,

$$S_K^2 = \left(\frac{\partial K}{\partial n}\right)^2 S_n^2 + \left(\frac{\partial K}{\partial I}\right)^2 S_I^2$$

$$= \frac{I^2}{n^2} S_n^2 + \frac{1}{n^2} S_I^2 \qquad (3.5.9)$$

where,

$$n = 6.65 \times 10^{12}/\text{litre}$$

$$I = 8.2 \times 10^{-12} \text{ Amp}$$

$$S_I^2 = (.01\ I)^2 = 67.2 \times 10^{-28} \text{ Amp}^2$$

Substituting the appropriate values into expression 3.5.9, we have $S_K^2 = 4 \times 10^{-52}$, $S_K = 2 \times 10^{-26}$ Amp-litre, and the percent standard error is 1.6%. Therefore, n can be determined accurately, if the spread of points on the I versus n plot is not greater than $\pm$ 1.6 percent of the best fit curve.

The critical measurement for this system is n_i. The smaller the standard error in n_i, the smaller the total error in α. The largest contributors to the error in α is $\left(\frac{\partial \alpha}{\partial n_i}\right)^2 S_{n_i}^2$ and $\left(\frac{\partial \alpha}{\partial n}\right)^2 S_n^2$ (S_n is dependent upon n_i). Since the measurement of n_i is the most important factor in determining the accuracy of α, a recorder should be used as the output instrument n_i to detect drift and average the signal over a period of time.

It will enable the investigator to determine S_{n_i} more precisely.

3.6 Experimental Procedure

The electron flourescence device can be calibrated with respect to n_i. Because of the number density ratio, the absolute value of n_i does not have to be known as accurately as the ratio.

The permanent magnet on the partial pressure gauge deflects the electron beam, and has to be removed prior to the tests. The partial pressure of nitrogen is obtained from a calibration of partial pressure of nitrogen against total pressure, made prior to operating the electron beam.

After the above calibration has been completed, the test surface can be cleaned, and the water circulated through the cooling jacket in chamber A.

The output current, I, from the photomultiplier is then calibrated against n_i, and by using expression 3.2.5 it can be calibrated against n. From the plot of I versus n, the value of K and S_K can be determined. The percent standard error in K must not be greater than 1.6%, if the desired accuracy for the measurement of n is to be attained.

A plot of I versus $n_i/n-n_{bg}$ can be made. In this case, n_i is the operating number density which remains constant throughout the experiment; n and n_{bg} are the experimental values.

Once the system has been calibrated no adjustment of the instrumentation can be tolerated.

CHAPTER IV

DISCUSSION

4.1 Comparison of Detectors

In both the ionization and electron flourescence detectors, the major source of error occurs in the measurement of n_i. It is imperative that S_{n_i} be minimized. A recorder can be used to average the output. This will reduce S_{n_i} provided there is no long term drift, either in the pressure or in the instrumentation.

The advantages of the ionization detector are; direct measurement of number density, and signal background ratio (n_{min}/n_{bg}) is approximately six.

The limiting factor is the x-ray limit of the ionization detector, and the background number density in chamber B.

The advantages of the electron flourescence detector are: the number density of nitrogen can be measured independently of impurity gases, and the electron beam does not disturb the molecular flight path.

The disadvantages of this device are: the signal intensity is low because photons emitted are collected by the photomultiplier and only a limited number of gases have emission spectra of sufficient intensity to be useable.

4.2 Modifications to the System

The baffle obstructing the conductance between chambers

B and C should be removed to insure that the effective pumping speed from chamber B is 1900 litres per second. Two smaller baffles can be placed over the titanium filament and the ion pump.

The MKS Baritron gauge has proven to be troublesome. Since the measurement of n_i is most important, it should be replaced by a more reliable gauge. A Varian Dual Range Ionization gauge which has a thoria-coated iridium filament (low work function), could be used to replace the Baritron gauge. This control unit has a long term drift of less than one percent.

The ionization detector is functional at the present time. However, a slight modification on the filament mounts would improve the convenience of replacing them.

The electron beam system should have the change in pressure gauge cited above as well as the following changes:

1. Light baffles could be placed around the electron beam except at point P. Baffles can reduce the photocurrent due to the excitation of the background molecules.

2. The orifice could be moved closer to the electron beam. If the distance d is reduced by half, the signal number density will subsequently be increased by four, and the photocurrent by the same amount.

3. If the effective electron beam current could be increased two fold, the photomultiplier output current will be increased proportionally.

4. A concave mirror could be placed opposite the lens

and point P. Point P can be placed at the focal point of the lens in the image of the mirror. This mirror will increase the effective solid angle of light received by the photomultiplier. For example a mirror with an effective area of 25 square inches placed 2 inches from point P would result in an increase in solid angle of approximately 24 times the solid angle obtained in reference (3).

These modifications will increase the calibration constant approximately 190 times the previous value. Therefore, the expected value of K would be 2.3×10^{-22} amp-litre, and the expected photomultiplier current would be 1.6×10^{-9} amps, which is three orders of magnitude larger than the photomultiplier dark current.

The analysis presented in Chapters II and III is only approximate, since the actual value for n corresponding to a given temperature T_s is not known. The actual values can not be known until the complete system is calibrated. Therefore, all the errors previously calculated are subjected to the dependence of n on T_s. However, these variations are not likely to be large.

Manufacturer's specifications for the control units previously mentioned all possess a long term drift of less than one percent. For any given instrument, the error associated with the measurement of n_i will probably be less than the error calculated in this study. Therefore, the actual error in α could be smaller than the error estimated in this study.

CHAPTER V

CONCLUSIONS

When using the ionization detector to measure α, the following sensitivities are associated with uncertainties in the parameters:

$$\left(\frac{\partial \alpha}{\partial G}\right)^2 S_G^2 = 0.001 \times 10^{-3}$$

$$\left(\frac{\partial \alpha}{\partial n_i}\right)^2 S_{n_i}^2 = 1.56 \times 10^{-3}$$

$$\left(\frac{\partial \alpha}{\partial n}\right)^2 S_n^2 = 3.07 \times 10^{-3}$$

$$\left(\frac{\partial \alpha}{\partial n_{bg}}\right)^2 S_{n_{bg}}^2 = 0.02 \times 10^{-3}$$

$$\left(\frac{\partial \alpha}{\partial \frac{T_s}{T_i}}\right)^2 S_{\frac{T_s}{T_i}}^2 = 0.22 \times 10^{-3}$$

The square of the standard deviation, S_α^2, is 4.86×10^{-3}. The percent standard error in α is 8.7% and the percent most probable error in α is 5.9%.

The square of the standard deviation in σ' (as determined from the ionization detector error analysis) is 3.1×10^{-3}. The percent standard error is 5.0% and the percent

most probable error is 4.7%.

The sensitivity of α has the following dependence when the electron flourescence detector is used:

$$\left(\frac{\partial \alpha}{\partial G_s}\right)^2 S_{G_s}^2 = 0.06 \times 10^{-3}$$

$$\left(\frac{\partial \alpha}{\partial n_i}\right)^2 S_{n_i}^2 = 1.56 \times 10^{-3}$$

$$\left(\frac{\partial \alpha}{\partial n}\right)^2 S_n^2 = 3.18 \times 10^{-3}$$

$$\left(\frac{\partial \alpha}{\partial n_{bg}}\right)^2 S_{n_{bg}}^2 = 0.003 \times 10^{-3}$$

$$\left(\frac{\partial \alpha}{\partial \frac{T_s}{T_i}}\right)^2 S_{\frac{T_s}{T_i}}^2 = 0.22 \times 10^{-3}$$

The square of the standard deviation in α is 5.02×10^{-3}. The percent standard error in α is 8.9%, and the percent most probable error is 6.0%.

The square of the standard deviation in σ', as determined from the electron flourescence detector error analysis, is 3.64×10^{-3}. The percent standard error is 7.5% and the percent most probable error is 5.0%.

This type of system is well suited for the measurement of thermal and normal momentum accommodation coefficients.

The experimental accuracy attained by using either detection system is approximately six percent. The major source of error occurs in the measurement of n_i.

BIBLIOGRAPHY

1. Wachman, H.Y., "The Thermal Accommodation Coefficient: A Critical Survey", J. Am. Rocket Soc., 32, (1962), 2-12.

2. Hurlbut, F.C., "On the Molecular Interactions Between Gases and Solids", University of California Tech. Report #HE-150-208, (1962).

3. Smyrl, G.S., "Electron Beam Measurements of Accommodation Coefficients", Masters Thesis at the University of Alberta, (1968).

4. Hagena, O.F., Scott, J.E. and Varma, A.K., "Design and Performance of an Aerodynamic Molecular Beam and Beam Detection System", Tech. Report NASA #AST-3038-103-674, (1967), 21-36.

5. Logan, R.M. and Stickney, R.E., "Simple Classical Model for the Scattering of Gas Atoms from a Solid Surface", J. Chem. Phys., 44, (1966), 195-201.

6. Hinchen, J.J. and Malloy, E.S., "Velocity of Molecular Molecules Scattered by Platinum Surfaces", United Aircraft Research Lab., (1966).

7. Parratt, L.G., "Probability and Experimental Errors in Science", Wiley and Sons, (1961), 111-116.

8. Gadamer, E.O., "Measurements of Density Distribution in a Rarefied Gas Flow Using the Flourescence Induced by a Thin Electron Beam", UTIAS Report #83, (1962).

9. Muntz, E.P., "Measurement of Rotational Temperature, Viabrational Temperature and Molecular Concentration in Non-Radiating Flows of Low Density Nitrogen", UTIAS Report #71, (1961), 8-9.

10. Marsden, D.J., "Measurement of Energy Transfer in Gas-Solid Surface Interactions Using Electron Beam Excited Emission of Light", UTIAS Report #101, (1964), 15-18.

11. Gadamer, E.O., Muntz, E.P. and Patterson, G.N., "Application of an Electron Gun for the Measurement of Density and Temperature in Rarefied Gas Flows", UTIAS Report #73, (1961).

12. Patterson, G.N., "Mechanics of Rarefied Gases and Plasmas", UTIAS Report #18, (1964), 2-92.

13. Lewin, G., "Fundamentals of Vacuum Science and Technology", McGraw-Hill, (1965).

14. Hartnett, J.P., "A Survey of Thermal Accommodation Coefficient", Sym. on Rarefied Gas Dyn., (1960), 1-28.

15. Rabinowicz, E., "An Introduction to Experimentation", Addison-Wesley (1970), 18-68.

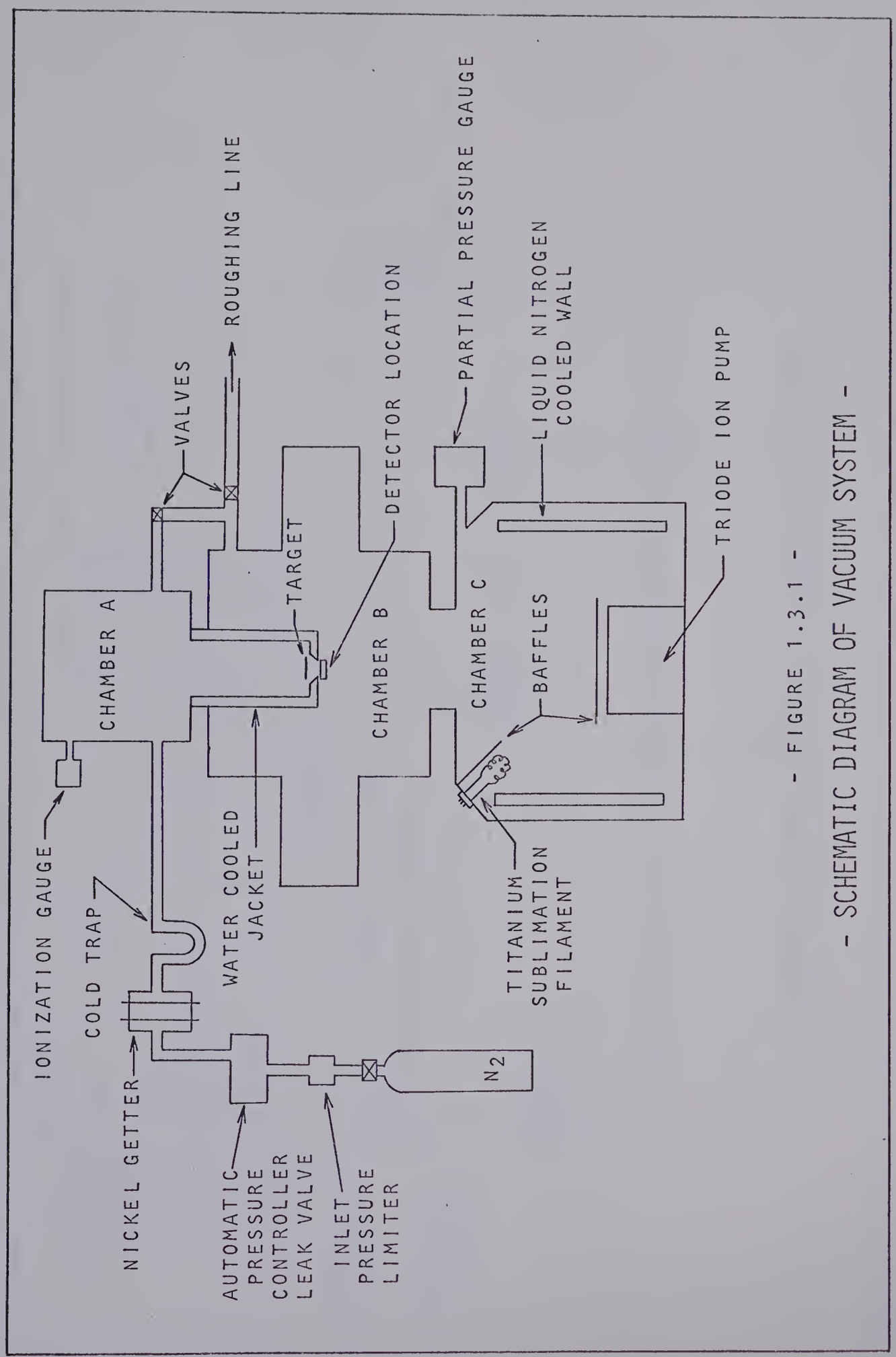

- FIGURE 1.3.1 -

- SCHEMATIC DIAGRAM OF VACUUM SYSTEM -

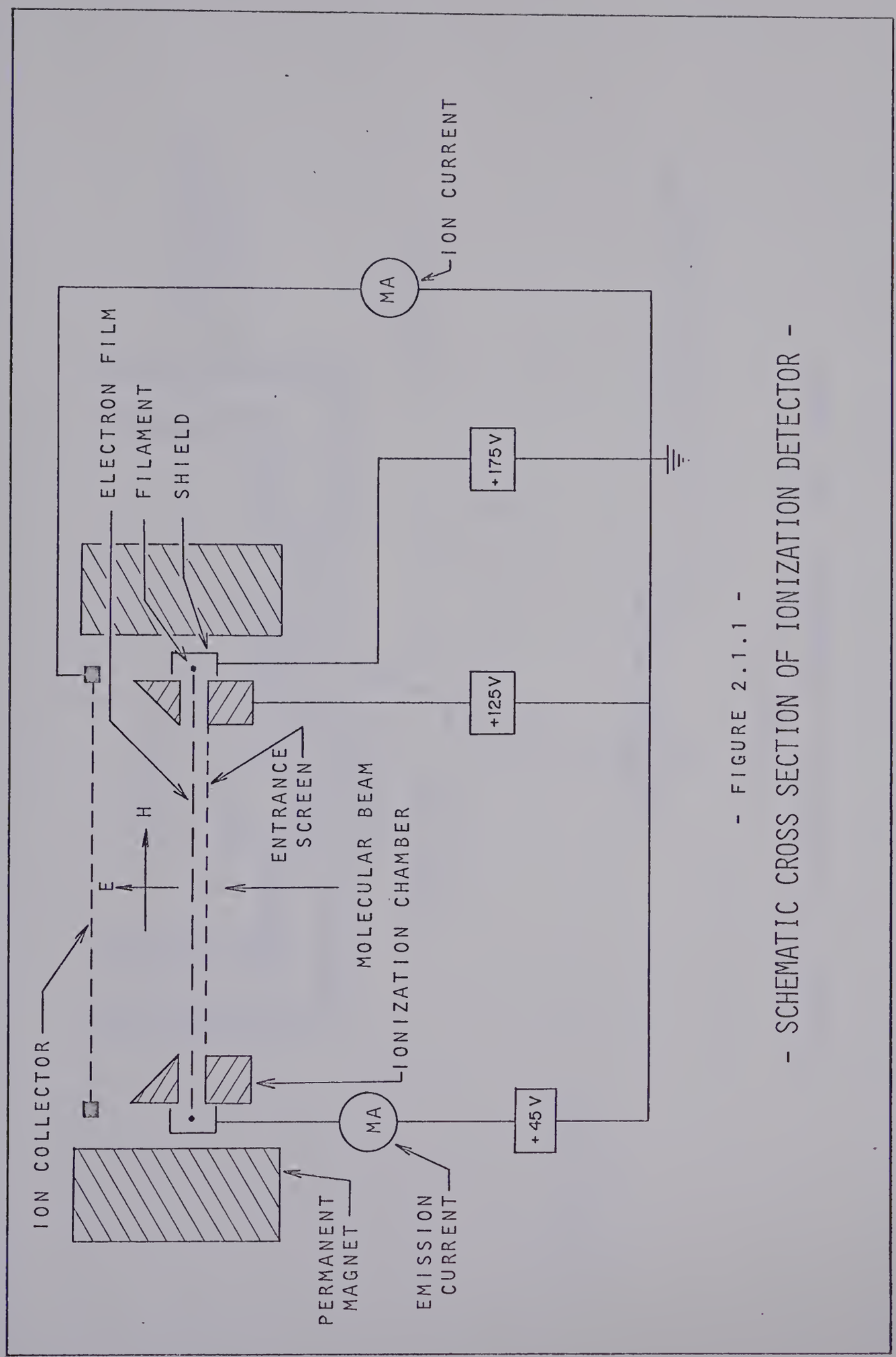

- FIGURE 2.1.1 -

- SCHEMATIC CROSS SECTION OF IONIZATION DETECTOR -

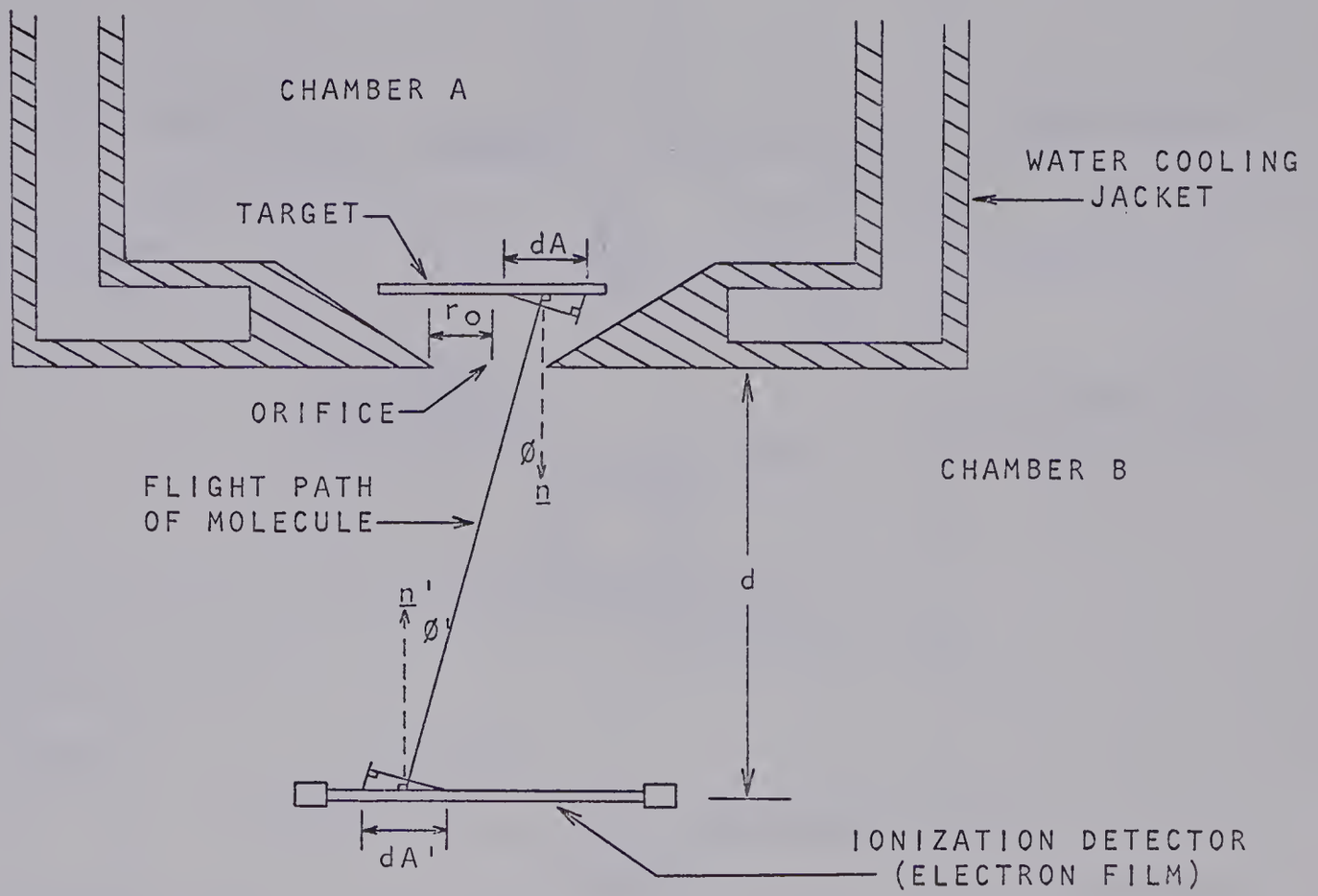

r_o = 0.1 cm.
d = 1.00 cm.

- FIGURE 2.2.1 -

- SCHEMATIC OF GEOMETRICAL ARRANGEMENT NEAR TARGET -

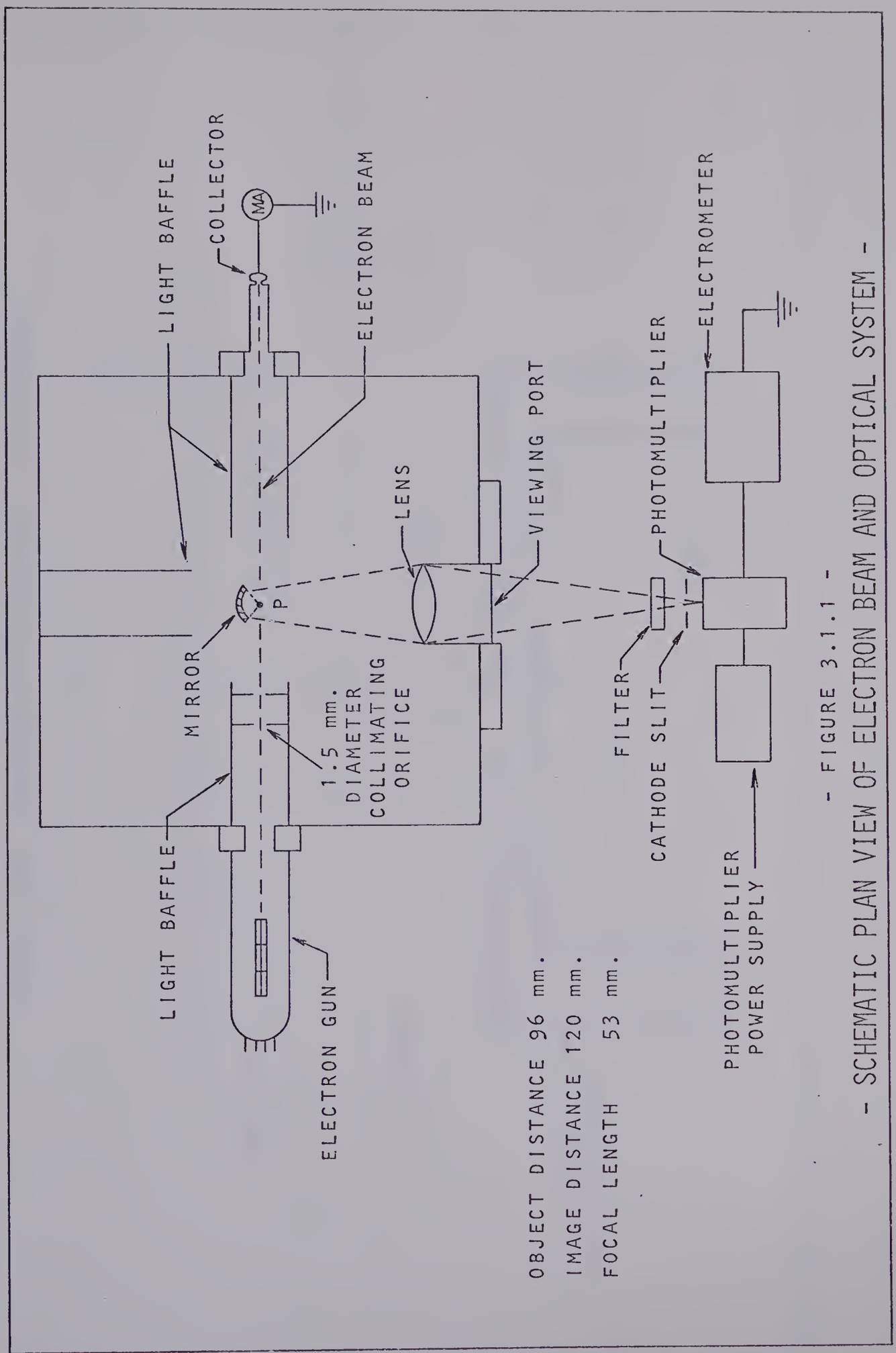

- FIGURE 3.1.1 -

- SCHEMATIC PLAN VIEW OF ELECTRON BEAM AND OPTICAL SYSTEM -

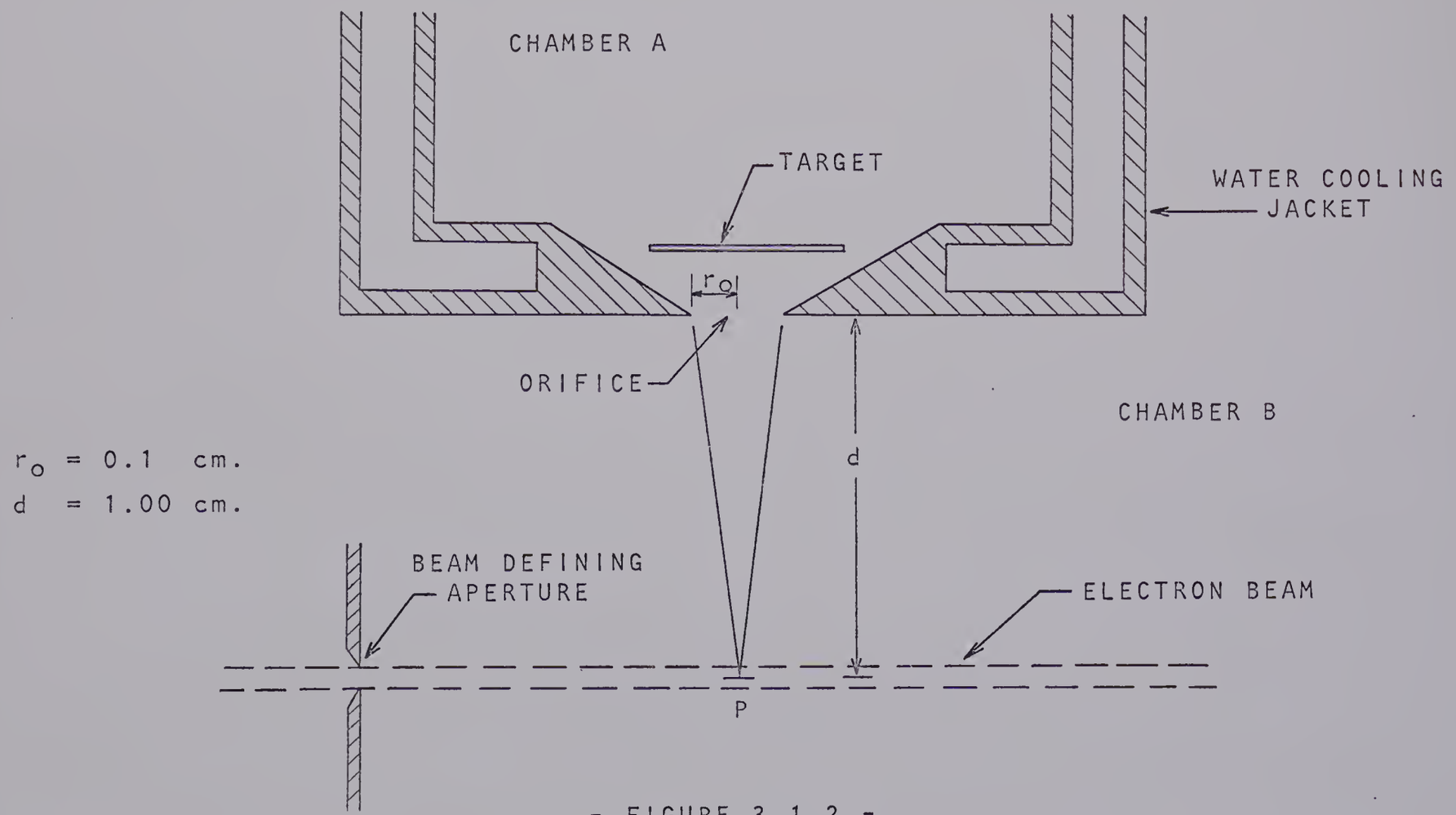

- FIGURE 3.1.2 -

SCHEMATIC OF GEOMETRICAL ARRANGEMENT NEAR TARGET -

B29942